RSC Advances

REVIEW

View Article Online
View Journal | View Issue

Cite this: *RSC Adv.*, 2017, **7**, 23573

MoS_2-DNA and MoS_2 based sensors

Lirong Yan,[a] Haixia Shi,*[b] Xiaowei Sui,[b] Zebin Deng[c] and Li Gao *[c]

Received 3rd March 2017
Accepted 20th April 2017

DOI: 10.1039/c7ra02649h

rsc.li/rsc-advances

MoS_2, a family member of transition-metal dichalcogenides, has shown highly attractive superiority for detection arising from its unique physical and chemical properties. Coupling MoS_2 with DNA recognition events leads to novel sensing platforms. Therefore, it has attracted increasing interest for MoS_2 based sensors in the increasing demands of biomedical applications. This has led to its rapid development in field of sensor. This paper summarizes the key issues in the development of MoS_2-DNA and MoS_2 based sensors related to fluorescence resonance energy transfer (FRET), electrochemical biosensing, and field effect transistors (FET) biosensing for use in the detection of DNA, proteins, metal ions, and others. The detection mechanisms and the advantages of MoS_2 are revealed. Future directions in which the field is likely to thrive and some critical challenges are also discussed.

1. Introduction

MoS_2 emerging two-dimensional-layered material analogous to graphene has been attracting much attention because of its unique physical and chemical properties, such as extraordinary thermal conductivity, robust mechanical properties, excellent nanoelectronics, unusual optical properties, and energy harvesting properties.[1] MoS_2 is a family member of transition-metal dichalcogenides. Each Mo is coordinated in a trigonal prismatic geometry to six S atoms; it is constructed by stacking covalently bound S–Mo–S through weak van der Waals interactions,[2] which aids in enhancing planar electric transportation properties.[3] MoS_2 nanosheets are able to adsorb single-stranded DNA by the van der Waals force between nucleobases and the basal plane of MoS_2 nanosheets.[1] Furthermore, MoS_2 nanosheets could be synthesized on a large scale and display strong fluorescence quenching properties in aqueous solution for sensing without further processing comparing with other nanomaterials such as graphene oxide.[4] MoS_2 shows the similar property and application with graphene oxide.[2,5,6] Therefore, MoS_2 has been widely applied in sensors that can detect DNA, proteins, metal ions, and other compounds. This paper provides an overview of the current approaches for sensors using DNA as recognition elements and their applications based on MoS_2. Future perspectives and some challenges are also discussed.

2. Synthesis of MoS_2

2.1. Exfoliation

Various methods have been reported about the synthesis of MoS_2 nanosheets, including scotch tape based micromechanical exfoliation,[7] spontaneous exfoliation,[8] chemical exfoliation,[9] ultrasound exfoliation,[10] liquid exfoliation,[11] and electrochemical exfoliation.[12] However, scotch tape based micromechanical exfoliation was limited to the fabrication of a small amount of single-layer nanosheet materials with low reproducibility.[13] Chemical exfoliation easily results in loss of the pristine semiconducting properties of MoS_2 due to structural changes that occur during Li intercalation.[9] Ultrasound exfoliation was possible to prepare MoS_2 nanosheets maintaining the semiconducting properties comparing with exfoliation using Li intercalation.[10] The liquid exfoliation was also easier to transfer the exfoliated products to arbitrary substrates avoiding complex transfer processes. The lateral size in electrochemical exfoliation of MoS_2 nanosheets was in the 5–50 μm range, which was much larger than that of chemically or liquid-phase exfoliated MoS_2 nanosheets.[12] Some improved methods have been reported, for example, the ethanol water mix-solvent sonication combined with grinding[14] and high power tip sonication.[15] Yao *et al.* also reported an effective grinding-assisted liquid exfoliation technique to achieve MoS_2 nanoflakes. However, this method was not scalable and the size and thickness of exfoliated flakes cannot be controlled.[16]

2.2. Chemical vapor deposition (CVD)

Ultrathin MoS_2 nanosheets were prepared by using exfoliation methods. With rapid development of study on MoS_2, the chemical vapor deposition (CVD) method generating large-area continuous MoS_2 films was in great demand. Kong proposed

[a]*Department of Gerontology, Affiliated Hospital of Jiangsu University, Zhenjiang 212001, P. R. China*

[b]*P. E. Department of Dalian Jiaotong University, Dalian 116028, P. R. China*

[c]*Institute of Life Sciences, Jiangsu University, Zhenjiang 212013, P. R. China. E-mail: gaoli@ujs.edu.cn*

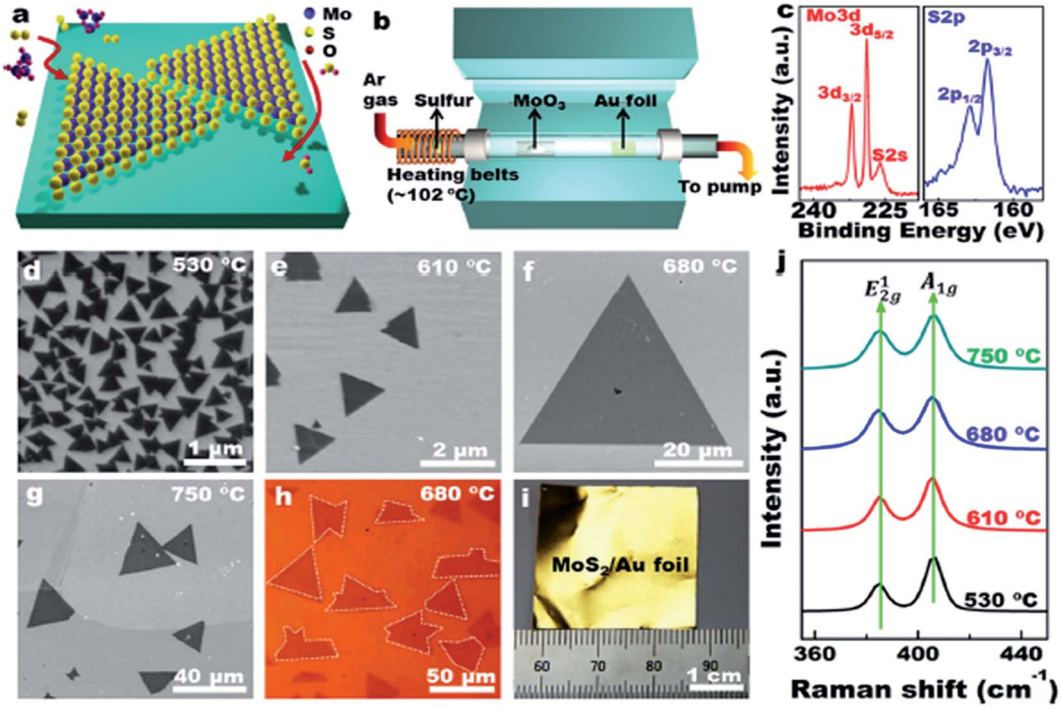

Fig. 1 LPCVD synthesis of monolayer MoS_2 on Au foils. Reprinted from Shi *et al.* (2014) with permission from American Chemical Society.

a novel chemical vapor deposition method to synthesize MoS_2 films with vertically aligned layers.[17] Wu *et al.* designed MoS_2 nanosheets with a high active site density by a microdomain method, and a high edge/basal ratio was obtained.[18]

Shi *et al.* demonstrated, for the first time, the scalable synthesis of monolayer MoS_2 on commercially available Au foils *via* a facile low-pressure CVD/(LPCVD) method (Fig. 1).[19] Wang *et al.* present an approach for synthesizing MoS_2 atomic layers with controlled shape and number of layers by the layer-by-layer surface sulfurization of MoO_2 microplates. The obtained MoS_2 flakes exhibited rhomboidal shape with lengths up to tens of micrometers that was larger than irregular flakes exfoliated from MoS_2 crystals.[20] It was a challenge to obtain crystalline MoS_2 thin film with controlled number of layers by CVD than

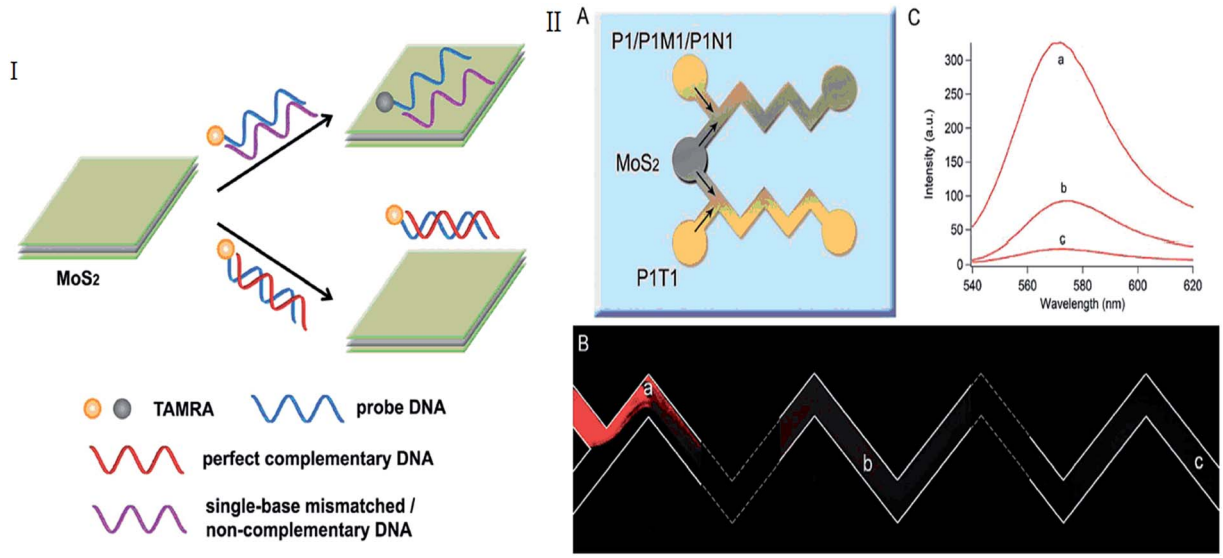

Fig. 2 (I) Schematic illustration of the MoS_2 nanosheet-based fluorometric DNA sensing assay. (II) (A) Design of a microfluidic detection scheme. Typical fluorescence image (B) and related fluorescence spectra (C) of P1 (100 nM) mixed with MoS_2 at the (a) start, (b) middle and (c) end of the microchannel. Reproduced from Huang *et al.* (2015) with permission from Royal Society of Chemistry.

graphene because no catalyst was involved in the growth of MoS_2. CVD has an advantage of growing uniform MoS_2 on a large scale. However, it is an expensive method and employs complicated procedures.[21] The synthesis of islands on the order of tens of nanometers grown by physical vapor deposition (PVD). It was difficult for achieving coverages in excess of 0.3 ML (monolayer) without compromising the structural quality of the MoS_2 that has been reported for the (111) faces of Cu[22] and Au.[23] Grønborg *et al.* present a growth method based on reactive PVD that solved this problem and permitted the growth of MoS_2 SL (single layer) with an almost unity coverage.[24]

2.3. Other methods

Various synthetic methods were explored in preparing MoS_2 nanomaterials with specific morphologies and unique properties, including gas-phase reactions or solid–gas,[25] thermal decomposition,[26] laser ablation,[27] sonochemical synthesis,[28] magnetron sputtering,[29] and electron beam irradiation activation.[30] However, the morphology and size of the products were hard to control. Compared with the other methods, hydrothermal synthesis was considered as an effective way to prepare inorganic nanomaterials in mild synthetic conditions.[31] Many types of MoS_2 micro/nano materials with various morphologies were made in the above approaches, such as nanotubes,[32] fullerene-like nanoparticles,[33,34] nanoplates,[35,36] nanorods,[37] nanowires,[38] nanoflowers,[39] and nanospheres,[40] nanoribbons,[41] nanoboxes[42] and hierarchical hollow cubic cages.[43] However, it was still a challenge to fabricate some novel structures of MoS_2 with the controlled morphologies in mild reaction conditions.[44] In addition, the scale up of current processes were limited because of expensive or corrosive precursors.

3. Detection using MoS_2-DNA based sensors

3.1. Detection based on FRET

MoS_2 monolayer shows dramatic improvement in photoluminescence quantum efficiency because of the specific 2D confinement of electron motion and the absence of interlayer perturbation. The improvement of photoluminescence in MoS_2 monolayer is also due to the fact that the monolayer, differently from few layer and bulk MoS_2, had a direct bandgap.[45–47] Compared with other nano-materials, except high fluorescent quenching efficiency, cheap bulk MoS_2 materials can be facilely synthesized in large scale and directly dispersed in aqueous solution.[1,48] When a ssDNA probe is absorbed on the surface of MoS_2, the nucleobases are buried between the densely negatively charged helical phosphate backbones. After combining with its target, this made weakly interact with the MoS_2 causing the dye-labeled probe is away from the surface of MoS_2.[2,49] This results in retention of the fluorescence of the probe. Therefore, MoS_2 nanosheets can act as efficient dye quenchers,[1,2] which have been employed to develop fluorescent sensing systems using DNA as recognition units (as shown in Table 1).

Huang *et al.* reported a novel MoS_2-based fluorescent biosensor for DNA detection *via* hybridization chain reactions (HCRs). The detection limit in this strategy was 15 pM.[50] Including DNA hybridization, Deng *et al.* described a simple signal-on fluorescence DNA methyltransferase (MTase) activity assay using a MoS_2 nanosheet. The Dam MTase activity can be quantified accordingly. Based on this assay, a linear range of 0.2–20 U mL^{-1} was achieved with high sensitivity and selectivity.[51] Huang *et al.* combined microfluidic biosensor for fluorescent DNA detection based on single-layered MoS_2 nanosheets (Fig. 2).[52] Yang *et al.* further present a novel microfluidic biosensor for sensitive fluorescence detection of DNA based on 3D architectural MoS_2/multi-walled carbon nanotube (MWCNT) nanocomposites.[53] Some label-free detection based on MoS_2-DNA sensors were also reported. In these papers, the probes without fluorescence were used and maybe lower the cost for detection. DNA oligonucleotides induced size control of layered MoS_2 was considered a label-free bioassay for the detection of single-nucleotide polymorphism.[54] Cao *et al.* developed a simple, low-cost and sensitive DNA sequences detection biosensor based on a label-free molecular beacon (MB) whose DNA hairpin structure terminal had a guanine-rich sequence that can enhance fluorescence of silver nanoclusters (Ag NCs). Even one nucleotide mismatched target can also be distinguished using this sensor.[55]

Many biological processes were related with the proteins. MoS_2-DNA based sensors were also developed to detect various proteins. Kong *et al.* proposed a novel aptamer-functionalized MoS_2 nanosheet fluorescent biosensor that detected PSA (as shown in Fig. 3). PSA was important for the early diagnosis of prostate cancer. The aptamer probe modified with FAM label at its 5′-terminal was absorbed on the surface of MoS_2. The fluorescence of the FAM-labeled aptamer was largely quenched owing to transfer of energy between the dye molecules and the MoS_2. In the presence of PSA, the FAM-labeled aptamer adopted a rigid structure owing to binding with the PSA. The affinity of

Table 1 Detection based on FRET[a]

Detected element	DNA probe	Donor, Exc/Em [nm]	MQE	Detection range or detection linear range	LOD	References
Target DNA	ssDNA	FAM, 494/520 nm	98%	0–15 nM	500 pM	Zhu *et al.* (2013)[2]
Target DNA	ssDNA	FAM, 490/520 nm	95%	0 to 200 pM	15 pM	Huang *et al.* (2015)[50]
Target DNA	ssDNA	TAMAR, 565/580 nm	90%	0 to 50 nM	0.5 fM	Huang *et al.* (2015)[52]
Disease-related genes	Hairpin loop DNA	AgNCs, 563/623 nm	90%	10 to 200 nmol	4.4 nmol	Cao *et al.* (2015)[55]
Dam activity	dsDNA	FAM, 495/518 nm	About 90%	0.2–20 U mL^{-1}	0.14 U mL^{-1}	Deng *et al.* (2015)[51]

[a] Exc, excitation; Em, maximum emission wavelength; MQE, maximum quenching efficiency; LOD, limit of detection.

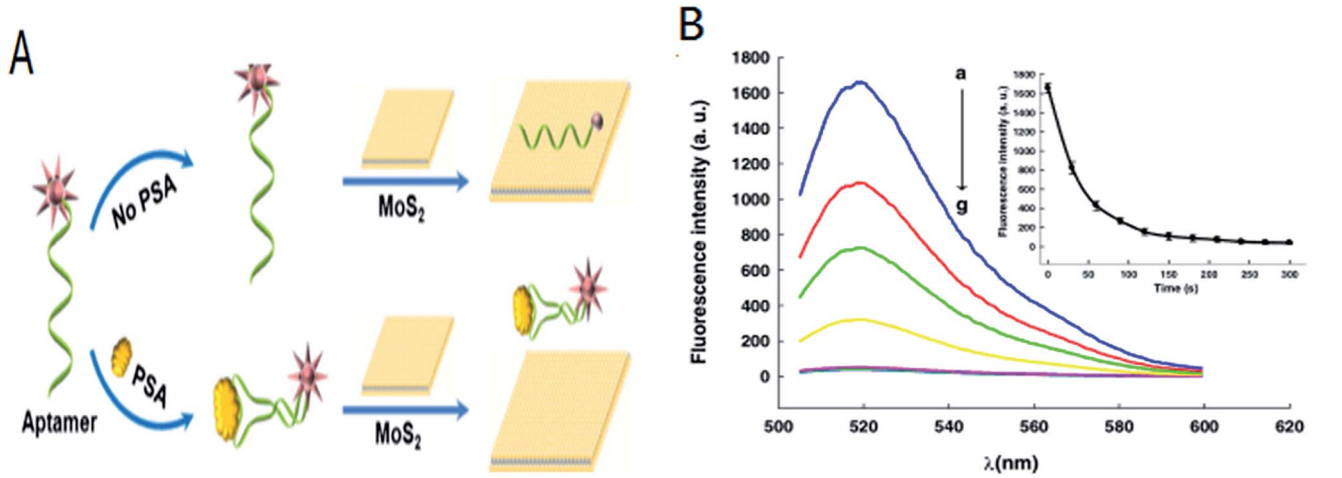

Fig. 3 (A) Schematic illustration of fluorescence sensing of PSA based on the aptamer-functionalized MoS_2 nanosheet biosensor, (B) fluorescence quenching of aptamer probe PA (50 nM) in the presence of an increasing amount of MoS_2 nanosheets (from (a to g) was 0, 5, 8, 10, 20, 30, and 40 μg mL^{-1}, respectively). Inset fluorescence quenching of PA (50 nM) by MoS_2 nanosheet. Reproduced from Long *et al.* (2015) with permission from Springer Publishing Group.

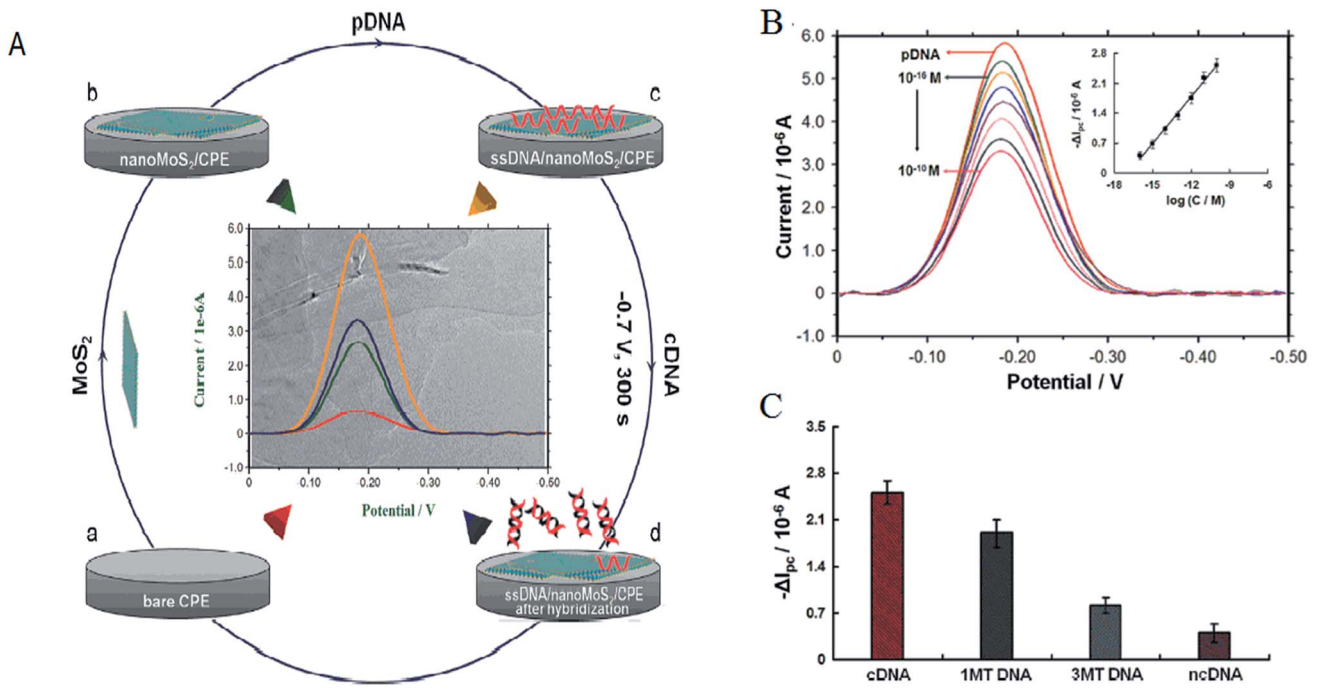

Fig. 4 (A) Schematic illustration of the label-free electrochemical DNA assay; (B) DPV plots of 2.0×10^{-5} M MB at pDNA (1.0×10^{-6} M) modified nanoMoS_2/CPE and that after hybridization with different concentrations of tlh gene sequence; (C) comparison with cDNA, single-base mismatched DNA, three-base mismatched DNA, and non-complementary DNA. Reproduced from Wang *et al.* (2015) with permission from Elsevier.

the aptamer with the MoS_2 decreased resulting in the release of the aptamer from the MoS_2 surface and the fluorescence signal was restored. PSA was detected with a limit of 0.2 ng mL^{-1}.[48] Ge *et al.* developed a novel fluorescence-activated MoS_2-DNA nanosheet biosensor for detecting proteins based on the self-assembled architecture of a DNA aptamer and a MoS_2 nanosheet.[1] In order to improve the sensitivity of detection, Xiang *et al.* combined the terminal protection of small-molecule-linked DNA and exonuclease III (Exo III)-aided DNA recycling amplification to detect protein based on MoS_2 nanosheet. In this method, protein was recycling used and resulted in the improvement of sensitivity for detection comparing with other methods. The detection limit was 0.67 ng mL^{-1} using the streptavidin (SA)-biotin system as a model.[56]

Detection of metal ions found in biological systems and in the environment was an attracted intense attention area of research. Mao *et al.* used for the first time single layer MoS_2 as the fluorescence quencher to design a detection method for Ag^+ with excellent robustness, selectivity and sensitivity. The detection limit in this assay was 1 nM for Ag^+.[57] Zhang

developed a novel fluorescent biosensor for uranyl ion (UO_2^{2+}) detection in aqueous environment based on the specific recognition of DNAzyme and MoS_2. The detection limit in this assay was 2.14 nM.[58]

3.2. Detection based on electrochemistry

Electrochemistry was an important tool for sensing. MoS_2 was quickly used to develop electrochemical DNA-based sensors. Some papers have reported electrochemical DNA-based sensors based on MoS_2 possess the exceptional physical and

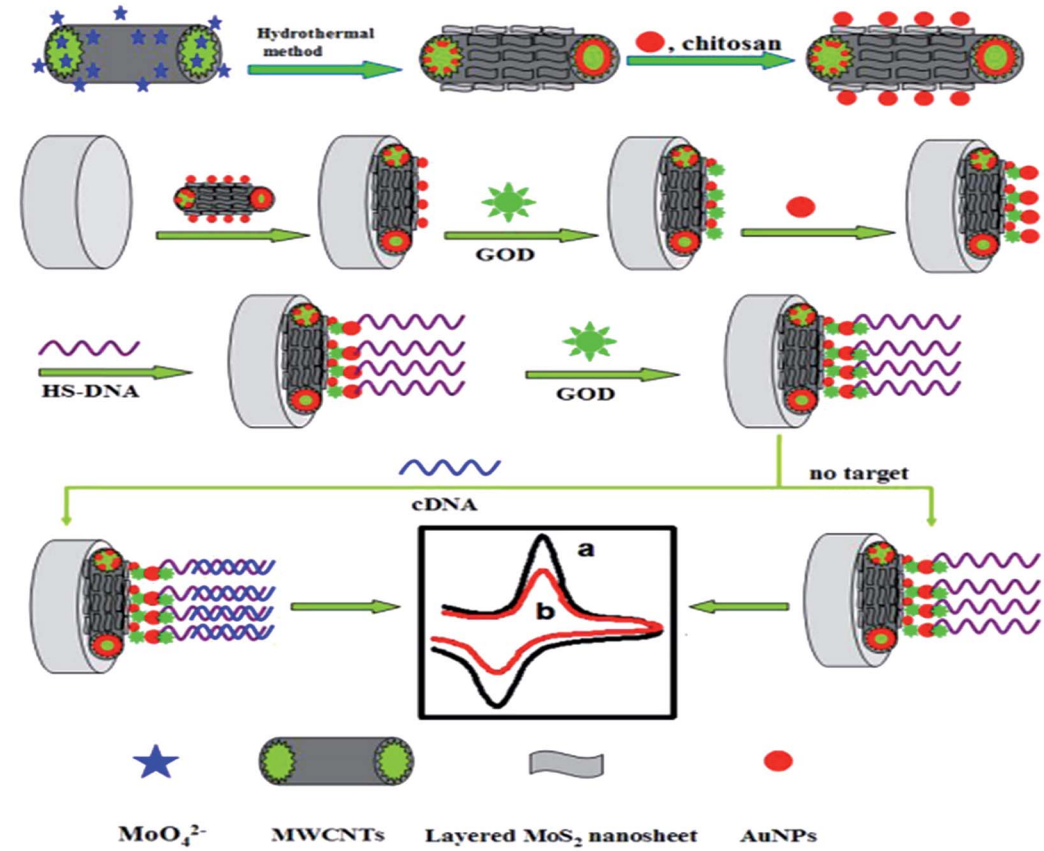

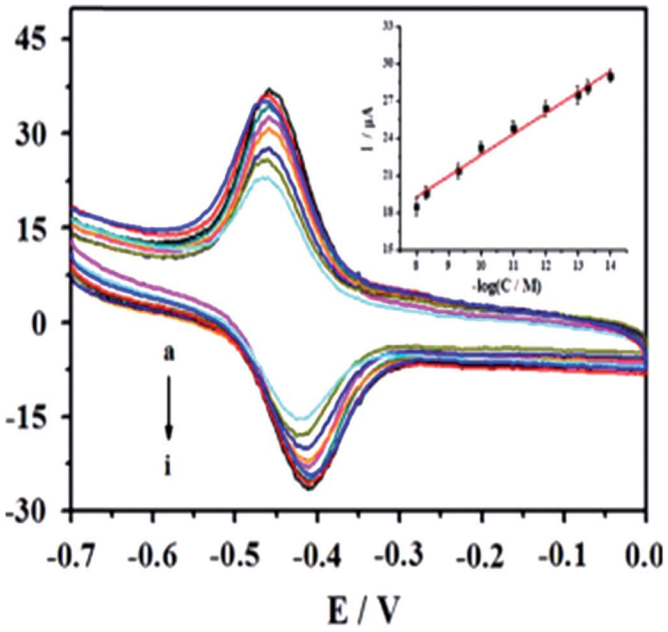

Fig. 5 (A) Schematic diagram of the electrochemical DNA biosensor; (B) the CVs of the proposed aptasensor after incubation in different concentrations of target ssDNA standard solution. Reproduced from Huang *et al.* (2014) with permission from Elsevier.

Table 2 Detection based on electrochemical sensors

Sensor materials	Detected element	Detection range or detection linear range	Detection limit	References
CdS–MoS_2 nanocomposites	IgE	0.001–10.0 nM	0.34 pM	Shi *et al.* (2015)[65]
MoS_2	DNA	1.0×10^{-16} M to 1.0×10^{-10} M	1.9×10^{-17} M	Wang *et al.*(2015)[60]
MoS_2–thionin composite	DNA	0.09 to 1.9 ng mL^{-1}	0.17 μA mL ng^{-1}	Wang *et al.* (2014)[62]
	RNA	10 ng mL^{-1} to 200 ng mL^{-1}	0.0022 μA mL ng^{-1}	
MoS_2/MWCNT	DNA	10 fM to 10^7 fM	0.79 fM	Huang *et al.* (2014)[3]
CdSe/ZnS quantum dots (QDs)–MoS_2	IgE	0.5 pM to 0.5 nM	0.18 pM	Liu *et al.* (2016)[66]
AuNPs–MoS_2 nanocomposites	ATP		0.74 nM	Su *et al.* (2016)[67]
	Thrombin		0.0012 nM	

electrochemical properties for detections. Loo *et al.* reported the principle of detection was based on the differential affinity of molybdenum disulfide nanoflakes towards single-stranded DNA and double-stranded DNA.[59] Based on the different affinity toward ssDNA *versus* dsDNA of the thin-layer MoS_2 nanosheets, Wang *et al.* performed the assay of tlh gene sequence from 1.0×10^{-16} M to 1.0×10^{-10} M with a detection limit of 1.9×10^{-17} M. The detection method described here was without labeling and the use of amplifiers, which resulted in the priority in sensitivity, simplicity, and costs. Furthermore, the proposed sensing platform could be extended to detect more targets (as shown in Fig. 4).[60]

Some functional materials have been decorated on MoS_2 to form MoS_2-based composite materials in order to further enhance the properties and broaden the applications of MoS_2. MoS_2-based composite materials have many significant advantages comparing with MoS_2. This maximized the advantages and minimized the drawbacks of the individual components. The composites can improve the sensitivity for DNA detection. Huang *et al.* constructed an ultrasensitive electrochemical DNA biosensor by assembling a thiol-tagged DNA probe on a MoS_2/MWCNT and gold nanoparticle (AuNP)-modified electrode coupled with glucose oxidase (GOD). The MoS_2/MWCNT composites film possessed large specific surface area and excellent biocompatibility. This increased the immobilization of GOD and enhanced the stability of the DNA probe. Moreover, the GOD membranes as tracer brought about higher current response and higher sensitivity. The detection signals were amplified (as shown in Fig. 5). The detection for DNA was down to 0.79 fM with a linear range from 10 fM to 10^7 fM. One-base mismatched DNA can be differentiated in this method.[3] Chu *et al.* made nano MoS_2/graphene composites by integrating nano MoS_2 and graphene through hydrothermal process and ultrasonic method. They developed an electrochemical circulating tumor DNA sensing platform based on this material. The cost and simplicity of the sensor preparation was decreased.[61] Including MoS_2 and materials (MWCNT and graphene) composites, MoS_2 and chemicals, such as polyaniline (PANI) and thionin that have some electrical conductivity, formed the composites improving the electrical property for high sensitivity. Wang *et al.* prepared a layered MoS_2–thionin composite to fabricate a double-stranded DNA (dsDNA) electrochemical biosensor. The linear range over dsDNA concentration from 0.09 ng mL^{-1} to 1.9 ng mL^{-1} was obtained. Moreover, single-stranded DNA (ssDNA) can be detected.[62] Yang *et al.* synthesized a PANI–MoS_2 nanocomposite based on ANI monomer and MoS_2. The PANI–MoS_2 nanocomposite with 0.054 g of MoS_2 can be considered as the optimal sensing platform for high sensitive DNA detection.[63] The sensitivity of detection based on MoS_2 and materials composites was higher comparing with MoS_2 and chemicals composites from publications. It maybe be electrochemical stability, more excellent electrocatalytic activity, and fast charge transfer rate.

The cooperative effects between MoS_2 and metal compounds paved the way to explore a variety of sensing applications. This can not only provide the couple sites with DNA but also improve the sensitivity of detection.[64] Proteins were also detected by using MoS_2 composites-based sensors. Immunoglobulin E (IgE) was one of important proteins. Shi *et al.* reported the CdS–MoS_2 composites immobilized on glassy carbon electrode surface as ECL emitter attached a complementary ssDNA (NH_2-ssDNA) of IgE. IgE aptamer (T-Apt) with DNAzyme-AuNPs hybridized with NH_2-ssDNA to form dsDNA. The DNAzyme with horseradish peroxidase-like activity could electrocatalyze the reduction of H_2O_2. The changed ECL intensity was proportional to concentration of IgE in the range of 0.001–10.0 nM with the detection limit of 0.34 pM (S/N = 3).[65] Liu *et al.* developed a novel competitive electrochemiluminescence (ECL) aptasensor based on CdSe/ZnS quantum dots (QDs) functionalized MoS_2 modified electrode for sensitive IgE detection using horseradish peroxidase (HRP) catalyzed biocatalytic precipitation (BCP) for signal quenching. This fabricated aptasensor displays a linear range from 0.5 pM to 0.5 nM with a detection limit of 0.18 pM (S/N = 3).[66] Liu *et al.*'s method had higher sensitivity than Shi *et al.*'s method. Other proteins were also reported by using MoS_2 composites-based sensors. Su *et al.* developed a MoS_2-based electrochemical aptasensor for the simultaneous detection of thrombin based on gold nanoparticles-decorated MoS_2 nanocomposites. This aptasensor could simultaneously determine thrombin as low as 0.0012 nM.[67] These results showed the signal amplification can be achieved by hybridizing MoS_2 with other components due to synergy effect. Therefore, the multifarious sensors have attracted more attention by some researchers as a new era (Table 2).

4. Detection based on MoS_2 sensors

The detection based on MoS_2 sensors were mainly using field-effect transistor (FET) that can offer a real-time and efficient

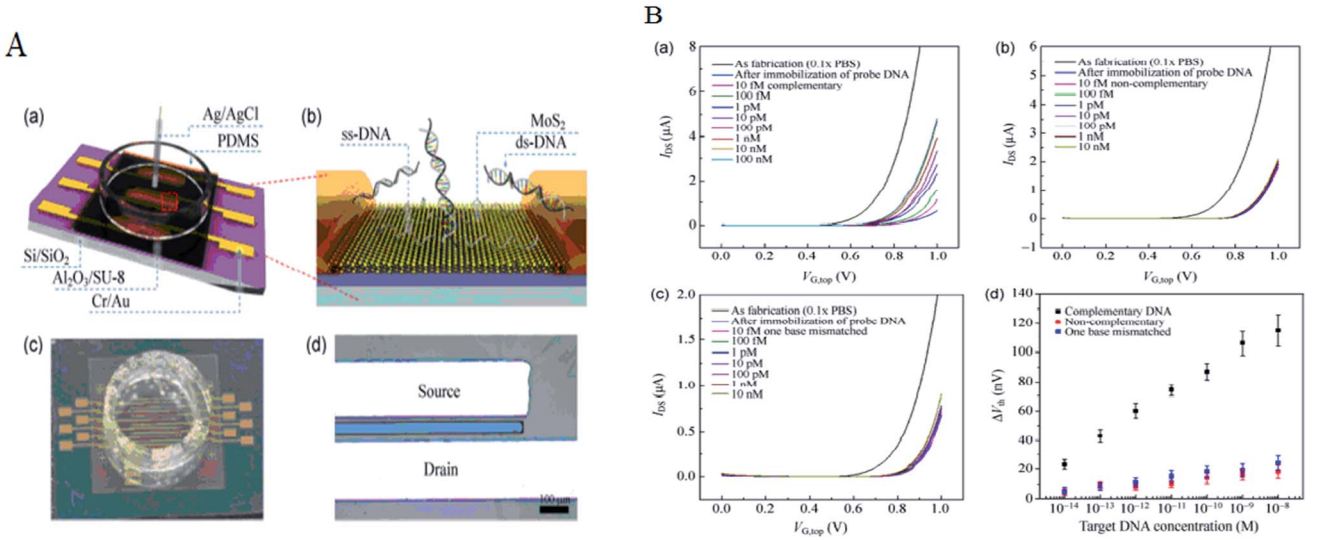

Fig. 6 (A) Schematic of MoS_2 FET and optical image of MoS_2 FETs; (B) transfer characteristics of MoS_2 FETs immobilized with the probe DNA molecules and hybridized with (a) complementary, (b) non-complementary, and (c) single-base mismatched DNA molecules. Reproduced from Lee *et al.* (2015) with permission from Springer Publishing Group.

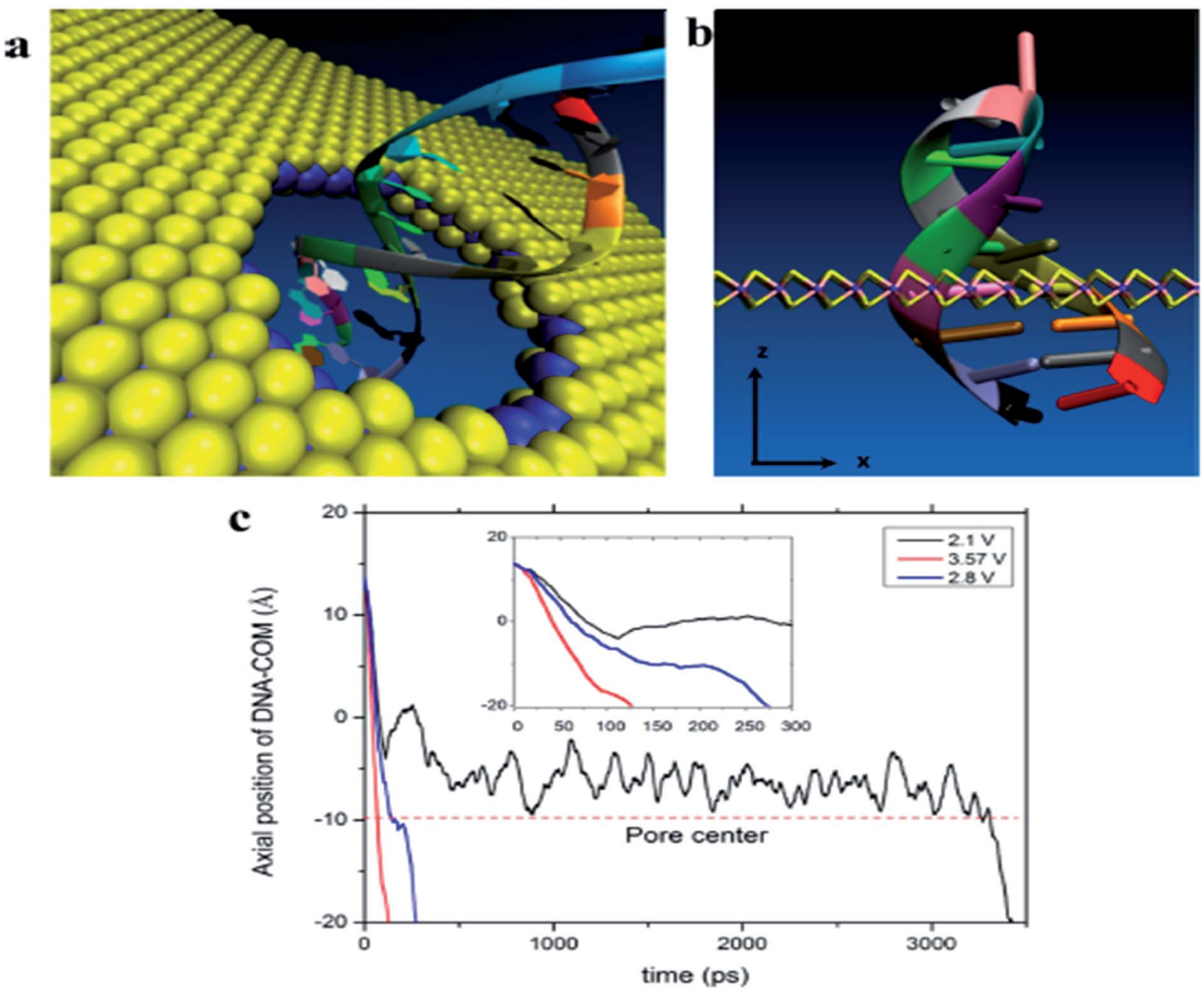

Fig. 7 (a) DNA translocation through a MoS_2 nanopore. (b) DNA hairpin structure with the loop at the top and the size view of MoS_2 fish-bone structure. (c) DNA translocation history for different biases. Reprinted from Farimani *et al.* (2014) with permission from American Chemical Society.

sensing platform for a variety of target analytes because of rapid electrical detection without fluorescence-labeling. Highly sensitive and rapid detection of biomolecules with a bioelectronic field-effect transistor was essential for clinical, military, or environmental applications.[68,69] FETs with two-dimensional (2D) nanomaterials attracted great attention owing to their many interesting electrical, optical, and mechanical properties.[70] MoS_2 with the bandgap is different from the pristine graphene. Single layer of MoS_2 has a large intrinsic bandgap of 1.8 eV.[71] Therefore, MoS_2 was applied in FET as a sensor. Lee *et al.* investigated a field-effect transistor (FET) with few-layer MoS_2 as a sensing-channel material for label-free detection of the hybridization of DNA molecules. Hybridization of DNA molecules adsorbed on the MoS_2 channel resulted in a shift of the threshold voltage in the negative direction and an increase in the drain current.[72] Lee *et al.* further demonstrated a non-volatile memory field-effect transistor (FET) for hybridization of single-stranded target DNA molecules with single-stranded probe DNA molecules physically adsorbed on the MoS_2 channel. This resulted in a shift of the threshold voltage (V_{th}) in the negative direction and an increase in the drain current because of the change in the surface charge density of the channel. The low detection limit was 10 fM in this method (as shown in Fig. 6).[73] Loan *et al.* first stacked graphene on a CVD MoS_2 to perform the differentiation of complementary and one-base mismatched DNA with the graphene/MoS_2 heterostructure. The concentration as low as 1 aM (10^{-18} M) can be detected.[70] Metal ion was also reported for detecting by FET. Zhou *et al.* reported a DNA-functionalized MoS_2 nanosheet/gold nanoparticle hybrid FET sensor for the ultrasensitive detection of Hg^{2+} in an aqueous environment. The sensor shows a rapid response (1–2 s) to Hg^{2+} and an ultralow detection limit of 0.1 nM.[74]

Some researchers focused on sequencing using MoS_2. The strong interaction between graphene and DNA and the high translocation velocity were the challenges for graphene nanopore on DNA sequencing. MoS_2 nanopore has shown promising potential for applications of DNA sequencing because MoS_2 is highly preferable to graphene in terms of DNA electronic base sensing. MoS_2 nanopore showed a distinct ionic current signal for single-nucleobase detection with a SNR of 15 using the simulation. The band gap of MoS_2 was significantly changed when bases are placed on the top of pristine MoS_2. DNA showed a nonsticky behavior and a more distinguishable signature per base using MoS_2 nanopore (as shown in Fig. 7).[75] Aluru *et al.* found that a single-layer MoS_2 was an extraordinary material (with a SNR > 15) for DNA sequencing by two competing technologies using atomistic and quantum simulations. A MoS_2 nanopore shows four distinct ionic current signals for single-nucleobase detection with low noise.[69] This can solve the problem that the noise increased in the detection process because the strong adsorption of DNA on graphene surface in graphene nanopore. Feng *et al.* further introduced a viscosity gradient system based on room-temperature ionic liquids (RTILs) to control the dynamics of DNA translocation through a nanometer-size pore fabricated in a thin MoS_2 membrane solving the high translocation velocity (3000–50 000 nt per m per s) of DNA molecules moving across such membranes limits their usability. This was the first time to statistically identify the DNA oligomer and the order of current of DNA oligomer was $poly(A)_{30}$ > $poly(T)_{30}$ > $poly(C)_{30}$ > $poly(G)_{30}$ when DNA oligomer translocates through the MoS_2 nanopore.[76] In addition, MoS_2 nanoribbon was also used for sequencing. Thomas analyzed the transmission of narrow semiconducting nanoribbons designed from MoS_2.[77] Smolyanitsky *et al.* proposed an aqueous functionalized molybdenum disulfide nanoribbon suspended over a solid electrode as a capacitive displacement sensor aimed at determining the DNA sequence. The results suggested a realistic, inherently base-specific, high-throughput electronic DNA sequencing device as a cost-effective *de novo* alternative to the existing methods.[78] However, the velocity of DNA passing through the nanopore and nanoribbon was too high in these experiments. It was still a challenge for achieving single-base resolution.

5. Conclusions and outlook

This paper provides a short history for MoS_2-DNA and MoS_2 based sensors. MoS_2, as a star among materials and widely studied by researchers worldwide, has drawn considerable interest in many fields. In this review, recent developments in MoS_2-DNA and MoS_2 based sensors for the detection of DNA, proteins, and heavy metal ions are described and discussed using their unique structure that contribute to their exceptional chemical and physical properties. Those properties lead to a broad range of applications in sensing. Some researchers have reported that MoS_2-DNA and MoS_2 sensors had relatively high sensitivity when compared with other nanomaterials; for example, the detection limitation based on MoS_2-DNA sensors for DNA was 0.5 fM (ref. 52) higher than 0.5 pM based on graphene oxide-DNA sensors.[79] MoS_2 is also highly preferable to graphene in terms of electronic-based sensing of DNA.[75] Therefore, this study helps to provide useful solutions related to some of the world's key problems, such as water and food security and the development of rapid and sensitive medical analysis methods.

Currently, the investigation of biosensing applications using MoS_2 is still in the early stage.

Some challenges related to sensing based MoS_2-DNA and MoS_2 remain and need to be resolved. (1) ssDNA is absorbed on the surface of MoS_2, and not all dsDNA can detach from the surface of MoS_2 after the complementary ssDNA, protein or other molecules combine to ssDNA. This hinders further improvement of the sensitivity of reported DNA sensors. (2) MoS_2, as a newly discovered material, faces some challenges including improving synthesis methods and extending its application in various fields. (3) MoS_2 properties such as the number of layers, sizes, morphology, functional groups and thickness influence the performance of DNA sensors, especially for electrochemical DNA sensors. (4) The large surface of low density MoS_2 in mass production may be difficult to handle, which can lead to health risks caused by inhaling and handling toxic reducing chemicals. (5) MoS_2 integrates with microfabrication techniques, such as current complementary metal oxide semiconductor (CMOS) technologies, which can increase

potential access for the development of label-free, low-cost and high-throughput detection arrays for sensing. However, the stability, selectivity and reproducibility of the devices based on MoS_2 should be further improved.

Acknowledgements

This work was supported by Jiangsu University (Grant no. 13JDG005), Natural Science Foundation of Liaoning Province (201601268), the Universities Natural Science Research Project of Jiangsu Province (Grant no. 15KJB180001), a project funded by the Priority Academic Program Development of Jiangsu Higher Education Institutions.

References

1 J. Ge, E. C. Ou, Q. R. Yu and X. Chu, *J. Mater. Chem. B*, 2014, **2**, 6255.
2 C. F. Zhu, Z. Y. Zeng, H. Li, F. C. Li, H. Fan and H. Zhang, *J. Am. Chem. Soc.*, 2013, **135**, 5998.
3 K. J. Huang, Y. J. Liu, H. B. Wang, Y. Y. Wang and Y. M. Liu, *Biosens. Bioelectron.*, 2014, **55**, 195.
4 A. Splendiani, L. Sun, Y. B. Zhang, T. S. Li, J. Kim, C. Y. Chim, G. Galli and F. Wang, *Nano Lett.*, 2010, **10**, 1271.
5 F. Li, Y. Huang, Q. Yang, Z. T. Zhong, D. Li, L. H. Wang, S. P. Song and C. H. Fan, *Nanoscale*, 2010, **2**, 1021.
6 C. H. Lu, J. Li, J. J. Liu, H. H. Yang, X. Chen and G. N. Chen, *Chem.–Eur. J.*, 2010, **16**, 4889.
7 B. Radisavljevic, A. Radenovic, J. Brivio, V. Giacometti and A. Kis, *Nat. Nanotechnol.*, 2011, **6**, 147.
8 L. Dong, S. Lin, L. Yang, J. J. Zhang, C. Yang, D. Yang and H. B. Lu, *Chem. Commun.*, 2014, **50**, 15936.
9 G. Eda, H. Yamaguchi, D. Voiry, T. Fujita, M. Chen and M. Chhowalla, *Nano Lett.*, 2011, **11**, 5111.
10 V. Šteng and J. Henych, *Nanoscale*, 2013, **5**, 3387.
11 K. M. Zhou, N. N. Mao, H. X. Wang, Y. Peng and H. L. Zhang, *Angew. Chem., Int. Ed.*, 2011, **50**, 10839.
12 N. A. Liu, P. Kim, J. H. Kim, J. H. Ye, S. Kim and C. J. Lee, *ACS Nano*, 2014, **8**, 6902.
13 Z. Y. Zeng, Z. Y. Yin, X. Huang, H. Li, Q. Y. He, G. Lu, F. Boey and H. Zhang, *Angew. Chem., Int. Ed.*, 2011, **123**, 11289.
14 Y. G. Yao, L. Tolentino, Z. Z. Yang, X. J. Song, W. Zhang, Y. S. Chen and C. P. Wong, *Adv. Funct. Mater.*, 2013, **23**, 3577.
15 R. J. Smith, P. J. King, M. Lotya, C. Wirtz, U. Khan, S. De, A. O'Neill, G. S. Duesberg, J. C. Grunlan, G. Moriarty, J. Chen, J. Z. Wang, I. M. Andrew, A. I. Minett, V. Nicolosi and J. N. Coleman, *Adv. Mater.*, 2011, **23**, 3944.
16 J. Y. Wu, M. N. Lin, L. D. Wang and T. Zhang, *J. Nanomater.*, 2014, **7**, 852735.
17 D. Kong, J. C. Wang, J. Cha, M. Pasta, K. J. Koski, J. Yao and Y. Cui, *Nano Lett.*, 2013, **13**, 1341.
18 Z. Z. Wu, B. Z. Fang, Z. P. Wang, C. L. Wang, Z. H. Liu, F. Y. Liu, W. Wang, A. Alfantazi, D. Z. Wang and D. P. Wilkinson, *ACS Catal.*, 2013, **3**, 2101.
19 J. P. Shi, D. L. Ma, G. F. Han, Y. Zhang, Q. Q. Ji, T. Gao, J. Y. Sun, X. J. Song, C. Li, Y. S. Zhang, X. Y. Lang, Y. F. Zhang and Z. F. Liu, *ACS Nano*, 2014, **8**, 10196.
20 X. S. Wang, H. B. Feng, Y. M. Wu and L. Y. Jiao, *J. Am. Chem. Soc.*, 2013, **135**, 5304.
21 J. H. Kim, J. Kim, S. D. Oh, S. Kim and S. H. Choi, *J. Korean Phys. Soc.*, 2015, **66**, 1852.
22 D. Kim, D. Sun, W. Lu, Z. Cheng, Y. Zhu, D. Le, T. S. Rahman and L. Bartels, *Langmuir*, 2011, **27**, 11650.
23 S. G. Sørensen, H. G. Füchtbauer, A. K. Tuxen, A. S. Walton and J. V. Lauritsen, *ACS Nano*, 2014, **8**, 6788.
24 S. S. Grønborg, S. Ulstrup, M. Bianchi, M. Dendzik, C. E. Sanders, J. V. Lauritsen, P. Hofmann and J. A. Miwa, *Langmuir*, 2015, **31**, 9700.
25 Y. Feldman, E. Wasserman, D. J. Srolovitz and R. Tenne, *Science*, 1995, **267**, 222.
26 C. M. Zelenski and P. K. Dorhout, *J. Am. Chem. Soc.*, 1998, **120**, 734.
27 J. J. Hu, J. S. Zabinski, J. H. Sanders, J. E. Bultman and A. A. Voevodin, *J. Phys. Chem. B*, 2006, **110**, 8914.
28 N. A. Dhas and K. S. Suslick, *J. Am. Chem. Soc.*, 2005, **127**, 2368.
29 K. Ellmer, R. Mientus, S. Seeger and B. V. Wei, *Phys. Status Solidi A*, 2004, **201**, 97.
30 M. Chhowalla and G. A. J. Amaratunga, *Nature*, 2000, **407**, 164.
31 W. J. Li, E. Shi and J. M. Ko, *J. Cryst. Growth*, 2003, **250**, 418.
32 J. Chen, S. L. Li, Q. Xu and K. Tanaka, *Chem. Commun.*, 2002, **16**, 1722.
33 H. Hwang, H. Kim and J. Cho, *Nano Lett.*, 2011, **11**, 4826.
34 K. Du, W. Fu, R. Wei, H. Yang, S. Liu, S. Yu and G. Zou, *Mater. Lett.*, 2007, **61**, 4887.
35 Z. Z. Wu, D. Z. Wang and A. K. Sun, *J. Cryst. Growth*, 2010, **312**, 340.
36 Z. Z. Wu, D. Z. Wang, X. Liang and A. K. Sun, *J. Cryst. Growth*, 2010, **312**, 1973.
37 M. A. Albiter, R. Huirache-Acuna, F. Paraguay-Delgado, J. L. Rico and G. Alonso-Nunez, *Nanotechnology*, 2006, **17**, 3473.
38 R. H. Wei, H. B. Yang, K. Dua, W. Y. Fu, Y. M. Tian, Q. J. Yu, S. K. Liu, M. H. Li and G. T. Zou, *Mater. Chem. Phys.*, 2008, **108**, 188.
39 G. G. Tang, J. R. Sun, C. Wei, K. Q. Wu, X. R. Ji, S. S. Liu, H. Tang and C. S. Li, *Mater. Lett.*, 2012, **86**, 9.
40 L. Ma, L. M. Xu, X. Y. Xu, Y. L. Luo and W. X. Chen, *Mater. Lett.*, 2009, **63**, 2022.
41 Q. Li, E. C. Walter, W. E. V. D. Veer, B. J. Murray, J. T. Newberg, E. W. Bohannan, J. A. Switzer, J. C. Hemminger and R. M. Penner, *J. Phys. Chem. B*, 2005, **109**, 3169.
42 S. Bastide, D. Dophil, J. P. Borra and C. Levy-Clement, *Adv. Mater.*, 2006, **18**, 106.
43 L. N. Ye, C. Z. Wu, W. Guo and Y. Xie, *Chem. Commun.*, 2006, **45**, 4738.
44 L. Ma, W. X. Chen, H. Li and Z. D. Xu, *Mater. Chem. Phys.*, 2009, **116**, 400.
45 M. Buscema, M. Barkelid, V. Zwiller, H. S. J. V. D. Zant, G. A. Steele and A. Castellanos-Gomez, *Nano Lett.*, 2013, **13**, 358.

46 K. P. Wang, J. Wang, J. T. Fan, M. Lotya, A. O'Neill, D. Fox, Y. Y. Feng, X. Y. Zhang, B. X. Jiang, Q. Z. Zhao, H. Z. Zhang, J. N. Coleman, L. Zhang and W. J. Blau, *ACS Nano*, 2013, **7**, 9260.
47 Q. H. Wang, K. Kalantar-Zadeh, A. Kis, J. N. Coleman and M. S. Strano, *Nat. Nanotechnol.*, 2012, **7**, 699.
48 R. M. Kong, L. Ding, Z. J. Wang, J. M. You and F. L. Qu, *Anal. Bioanal. Chem.*, 2015, **407**, 369.
49 H. D. Ha, D. J. Han, J. S. Choi, M. T. Park and S. Seo, *Small*, 2014, **10**, 3858.
50 J. H. Huang, L. Ye, X. Gao, H. Li, J. B. Xu and Z. G. Li, *J. Mater. Chem. B*, 2015, **3**, 2395.
51 H. M. Deng, X. J. Yang and Z. Q. Gao, *Analyst*, 2015, **140**, 3210.
52 Y. X. Huang, Y. M. Shi, H. Y. Yang and Y. Ai, *Nanoscale*, 2015, **7**, 2245.
53 D. H. Yang, M. Tayebi, Y. X. Huang, H. Y. Yang and Y. Ai, *Sensors*, 2016, **16**, 1911.
54 B. L. Li, H. L. Zou, L. Lu, Y. Yang, J. L. Lei, H. Q. Luo and N. B. Li, *Adv. Funct. Mater.*, 2015, **25**, 3541.
55 Q. Cao, Y. Teng, X. Yang, J. Wang and E. Wang, *Biosens. Bioelectron.*, 2015, **74**, 318.
56 X. Xiang, J. B. Shi, F. H. Huang, M. M. Zheng, Q. C. Deng and J. Q. Xu, *Biosens. Bioelectron.*, 2015, **74**, 227.
57 K. Mao, Z. T. Wu, Y. R. Chen, X. D. Zhou, A. G. Shen and J. M. Hu, *Talanta*, 2015, **132**, 658.
58 H. Y. Zhang, Y. J. Ruan, L. Lin, M. G. Lin, X. X. Zeng, Z. M. Xi and F. F. Fu, *Spectrochim. Acta, Part A*, 2015, **146**, 1.
59 A. H. Loo, A. Bonanni, A. Ambrosi and M. Pumera, *Nanoscale*, 2014, **6**, 11971.
60 X. X. Wang, F. X. Nan, J. L. Zhao, T. Yang, T. Ge and K. Jiao, *Biosens. Bioelectron.*, 2015, **64**, 386.
61 Y. L. Chu, B. Cai, Y. Ma, M. G. Zhao, Z. Z. Ye and J. Y. Huang, *RSC Adv.*, 2016, **6**, 22673.
62 T. Y. Wang, R. Z. Zhu, J. Q. Zhuo, Z. W. Zhu, Y. H. Shao and M. X. Li, *Anal. Chem.*, 2014, **86**, 12064.
63 G. H. Zhou, J. B. Chang, H. H. Pu, K. Y. Shi, S. Mao, X. Y. Sui, R. Ren, S. M. Cui and J. H. Chen, *ACS Sens.*, 2016, **1**, 295.
64 M. Khan, M. N. Tahir, S. F. Adil, H. U. Khan, M. R. H. Siddiqui, A. A. Al-warthan and W. Tre- mel, *J. Mater. Chem.*, 2015, **3**, 18753.
65 G. F. Shi, J. T. Cao, J. J. Zhang, Y. M. Liu, Y. H. Chen and S. W. Ren, *Sens. Actuators, B*, 2015, **220**, 340.
66 Y. M. Liu, J. J. Yang, J. T. Cao, J. J. Zhang, Y. H. Chen and S. W. Ren, *Sens. Actuators, B*, 2016, **232**, 538.
67 S. Su, H. F. Sun, W. F. Cao, J. Chao, H. Z. Peng, X. L. Zuo, L. H. Yuwen, C. H. Fan and L. H. Wang, *ACS Appl. Mater. Interfaces*, 2016, **8**, 6826.
68 M. S. Makowski and A. Ivanisevic, *Small*, 2011, **7**, 1863.
69 D. Sarkar and K. Banerjee, *Appl. Phys. Lett.*, 2012, **100**, 143108.
70 P. T. K. Loan, W. J. C. Zhang, T. Lin, K. H. Wei, L. J. Li and C. H. Chen, *Adv. Mater.*, 2014, **26**, 4838.
71 K. F. Mak, C. Lee, J. Hone, J. Shan and T. F. Heinz, *Phys. Rev. Lett.*, 2010, **105**, 136805.
72 D. W. Lee, J. Lee, Y. Sohn, B. Y. Kim, Y. M. Son, H. Bark, J. Jung, M. Choi, T. H. Kim, C. Lee and N. E. Lee, *Nano Res.*, 2015, **8**, 2340.
73 J. Lee, S. W. Min, H. S. Lee, Y. Yi and S. Yim, *J. Mater. Chem. C*, 2014, **2**, 5411.
74 T. Yang, L. Meng, H. Y. Chen, S. Z. Luo, W. H. Li and K. Jiao, *Adv. Mater. Interfaces*, 2016, **3**, 1500700.
75 A. B. Farimani, K. Min and N. R. Aluru, *ACS Nano*, 2014, **8**, 7914.
76 J. D. Feng, K. Liu, R. D. Bulushev, S. Khlybov, D. Dumcenco, A. Kis and A. Radenovic, *Nat. Nanotechnol.*, 2015, **10**, 1070.
77 S. Thomas, A. C. Rajan, M. R. Rezapour and K. S. Kim, *J. Phys. Chem. C*, 2014, **118**, 10855.
78 A. Smolyanitsky, B. I. Yakobson, T. A. Wassenaar, E. Paulechka and K. Kroenlein, *ACS Nano*, 2016, **10**, 9009.
79 L. Peng, Z. Zhu, Y. Chen, D. Han and W. H. Tan, *Biosens. Bioelectron.*, 2012, **35**, 475.

